WRF forecasts over the Southeast United States: Does a larger domain lead to better results?

Ligia R. Bernardet[1&%], Peter Bogenschutz[2*], John Snook[13♣], Andrew Loughe[14]

[1]NOAA Research – Forecast Systems Laboratory, Boulder, CO
[2] *The Florida State University*, Department of Meteorology, Tallahassee, FL
[3] ATMET LLC
[4] Cooperative Institute for Research in Environmental Sciences, University of Colorado, Boulder, CO

I. Introduction

Under the auspices of a continuing nationwide effort led by NOAA, known as the Coastal Storms Initiative (CSI), the Weather Research and Forecasting (WRF) modeling framework is being utilized as a tool to improve forecasts of Southeast United States precipitation, coastal winds, and visibility. The first initiative of the CSI project involved the installation of the Advanced Research core WRF model (ARW) operationally at the Jacksonville, FL (JAX) National Weather Service (NWS) Weather Forecast Office (WFO) in May 2003, which involved both an Eta initialized simulation as well as a local data assimilation component (Shaw et. al. 2004). Bogenschutz et. al. (2005) showed that both simulations of the WRF model, despite a cool afternoon surface temperature bias, were able to increase forecast accuracy of visibility, precipitation, sea breeze detection and convection compared to the Eta 12-km model (218 grids).

This component of the initiative seeks to address whether a CONUS size WRF domain, since it removes the lateral boundaries from the region of interest, can add forecast accuracy compared to the JAX WRF domain. Differences in forecasts of surface and upper air variables, precipitation, and sea breezes will be examined for each domain. Model verification for precipitation and sea breezes will utilize the Ebert & McBride (Ebert and McBride 2000) and Contour Error Mapping techniques (Case et al. 2002) to gain a better understanding of model performance and comparison. This study will run from 1 April to 30 June, 2005, but in this paper only results for April will be presented.

II. Experiment Setup

This experiment used the Nonhydrostatic Mesoscale Model (NMM) core of the WRF model (Janjic 2003), which runs on a rotated lat-lon projection using E-grid staggering. The horizontal grid spacing is 5 km and 38 levels are employed in the vertical. Figure 1 shows the two domains used: the large domain covers the CONUS and the small domain covers the area of responsibility of the JAX NWS office. Apart from the extension of the horizontal domain, the two setups were identical. Both forecasts were initialized at 0000 UTC from the Eta 212 analysis and ran for 48 h. The physical parameterizations used were:

- Land-surface model: NOAH unified 5-layer.
- Microphysics: Ferrier.
- Cumulus parameterization: none.
- Planetary Boundary Layer (PBL): Mellor-Yamada-Janjic 2.5.
- Shortwave radiation: Lacis-Hansen, used in the operational Eta model.
- Longwave radiation: Fels-Schwartzkopf, used in the operational Eta model.

The runs over the CONUS domain are a springtime extension of the Developmental Testbed Center (DTC) Winter Forecast Experiment (DWFE) (Nance et al. 2005). Following the DTC end-to-end process, the forecasts from both domains were post-processed using the NCEP WRF Post-Processing Software (Chuang et al. 2004) to be de-staggered, interpolated vertically to isobaric levels and interpolated horizontally to a Lambert conformal grid. Finally, verification statistics from both models were computed over a common grid, similar to the WRF-CSI domain.

A. *Verification*

The surface and upper verification was performed using the WRF Verification System, developed at the National Centers for Environmental Prediction (NCEP) and NOAA Forecast Systems Laboratory (FSL). In this system the forecasts are first interpolated to station location and then compared to the observations. METAR and conventional radiosondes are used for surface and upper air observations, respectively.

Precipitation verification is performed using the Ebert & McBride Technique (EMT). The EMT automatically detects and verifies individual precipitation entities, or contiguous rain areas (CRAs), in both the forecast and observation grids. Shifting the forecast rain entity to achieve a maximum correlation coefficient with the observations allows an evaluation for that entity

[&]Contract with Systems Research Group, Inc. (SRG), Colorado Springs, Colorado
% Also affiliated with the Developmental Tested Center, Boulder, CO
[♣]Contract with Systems Research Group, Inc. (SRG), Colorado Springs, Colorado and NOAA Forecast Systems Laboratory
[*]Corresponding author address: Peter Bogenschutz, Department of Meteorology, Florida State University, Tallahassee, FL 32309 email: pbogen@met.fsu.edu

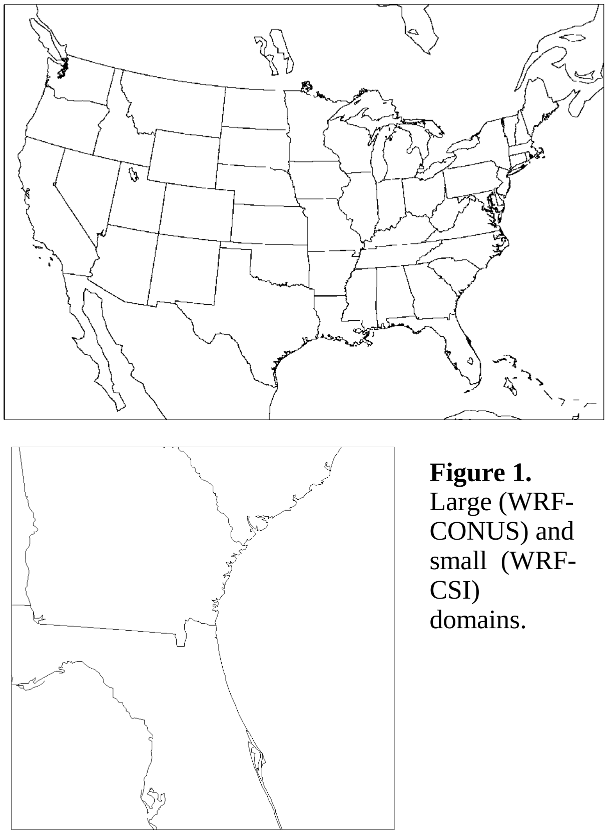

Figure 1. Large (WRF-CONUS) and small (WRF-CSI) domains.

assuming no displacement error. This is advantageous for mesoscale forecasts where a minor mislocation error of the forecast entity will likely lead to statistics representing little skill for the model. After the forecast entity is shifted, an error decomposition can be computed, consisting of error due to displacement, pattern, and volume. Stage IV precipitation data, provided by NCEP and the River Forecast Centers, are used as the observational data. Both the WRF CONUS and JAX domains are assessed for two periods of 24-h accumulation for each model run, 0-–24 h and 24-–48 h forecast hours. The minimum threshold for a CRA to be defined is set at 0.25 in. In addition, the shifted forecast entity must be correlated at the 95% confidence interval for the CRA to be counted as a hit.

III. Results

A. Temperature & Relative Humidity

April surface temperature verification (2m observations) shows that the WRF-CONUS holds a slight advantage over the WRF-CSI for the first 39 forecast hours. The differences between the two setups are maximized during the 15^{th}-–27^{th} forecast hours, or the time of maximum heating for the first 24-h cycle, when the WRF-CSI tends to overforecast (Figure 2). However, during the final forecast hours (39-48) the WRF-CONUS suffers from a cool surface temperature bias and exhibits higher errors than the WRF-CSI. Hence, while both models hold similar forecasts during the nighttime hours, differences are seen during the day which favors the WRF-CONUS for the first 24 h and the WRF-CSI for the latter. While both models overforecast/underforcast surface relative humidity during the daytime/nighttime, respectively, these errors are maximized by the WRF-CONUS near the end of the cycle with relative humidity errors on the magnitude of 19% (not shown).

For many of the upper levels, temperature forecasts are similar between the domains, with the lowest RMSE occurring near the 500-–400 hPa layer and the maximum errors near the top of the model at 150hPa, where both models tend to underforecast temperature by approximately 1.5-–2.0 K in an average for all forecast periods. The most notable difference between the models occurs at 700 hPa, where the WRF-CSI tends to underforecast temperature while the WRF-CONUS slightly overforecasts. These findings are an improvement over those found in the original CSI experiment, where the WRF model (ARW version 1.3) routinely overforecast temperature at the top of the boundary layer by 1-–2 K, which typically modeled a stable atmosphere stratus cloud cover, as opposed to the usual scattered cumulus fields, that resulted in the cool surface temperature bias (Bogenschutz et al. 2004).

B. Vector Wind

For surface wind forecasts, both the WRF-CONUS and WRF-CSI are comparable for the month of April, with the largest difference of RMSE between the two setups occurring at the 42^{nd} forecast hour of 0.25 m s^{-1}. Both models experience their largest errors during the daytime hours, with an average error of 3.40 m s^{-1} at the 21^{st} forecast hour. The WRF-CONUS holds a slight advantage over the WRF-CSI for the daytime hours, while both models perform similarly during the nighttime. At all forecast hours both models tend to overforecast surface wind speed.

Both the WRF-CONUS and WRF-CSI models underforecast wind speed below 100 hPa. The WRF-CONUS generally holds the smaller biases at the lower levels (below 400 hPa), while the WRF-CSI generally exhibits smaller biases near the jet region, although the advantage of the WRF-CONUS at the surface is more substantial.

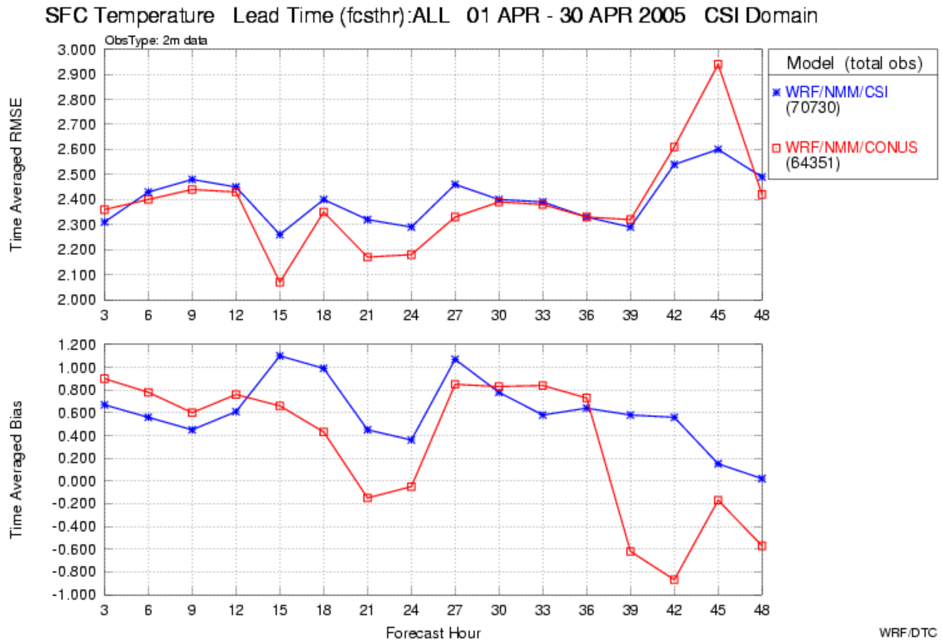

Figure 2. Temperature bias and RMSE statistics at each forecast hour for April for WRF-CONUS and WRF-CSI.

C. Sea Level Pressure

With exception of the 12th–18th forecast hours, the WRF-CONUS holds a slight statistical advantage over the WRF-CSI for April sea level pressure (SLP). RMSE differences between the two setups are small, typically 0.075 hPa with a maximum error difference of 0.20 hPa at the 6th forecast hour. Both models overforecast SLP for the average of every forecast hour for April, with maximum errors during the nighttime hours.

D. Precipitation

For April a total of 50 CRAs are detected through observations. The WRF-CONUS correctly forecasts 44 of these CRAs with 6 false alarms, while the WRF-CSI forecasts 48 of these CRAs along with 9 false alarms. This translates to a Critical Success Rate (CSR) of 0.79 and 0.81, respectively. Of the 44 CRAs forecast by the WRF-CONUS, 100% occupied 100 or more grid points, while all 6 missed CRAs contained less than 100 grid points. Of the 48 CRAs forecast by the WRF-CSI, five contained less than 100 grid points , as well as one missed event. Most of the precipitation for this month is driven by synoptic scale forcing, along with a few convective pop-up thunderstorm entities.

While the WRF-CSI has a higher hit rate, the WRF-CONUS exhibits more desirable correlation, displacement, RMS error, and rain rate scores for events where both models forecast a CRA hit. Though the average correlation coefficients for a shifted forecast are close (0.49 and 0.44 for WRF-CONUS and WRF-CSI, respectively), the differences in correlations for an unshifted forecast have more spread, with 0.18 for the WRF-CSI and 0.34 for the WRF-CONUS. This suggests larger displacement errors for the WRF-CSI, which exhibits an average displacement of 1.0°, compared to the WRF-CONUS average displacement of 0.612°. Both models overforecast the precipitation volume of the CRAs, with average rain rates during 24 hr of 0.60 in and 0.53 in for the WRF-CSI and WRF-CONUS, respectively, compared to the observed value of 0.39 in the same period. Systematic error decomposition for both models can be seen in Figure 3. Most notable is the difference in displacement error between the WRF-CSI and WRF-CONUS models.

The WRF-CSI forecasted five small CRAs (containing fewer than 100 grid points) but the WRF-CONUS did not. All five of these CRAs occurred well inland and are most likely the result of convection from afternoon heating. It is also important to note that the WRF-CSI occasionally forecasted noise at the edge of the boundaries, resulting in forecasts of small but intense entities with rainfall amounts greater than 15 in during 24 hr. This accounts for half of the false alarm instances associated with the WRF-CSI for April.

IV. Discussion and conclusions

Preliminary investigation for the WRF-CONUS and WRF-CSI for April statistically yields similar results in terms of temperature, wind, and sea level pressure

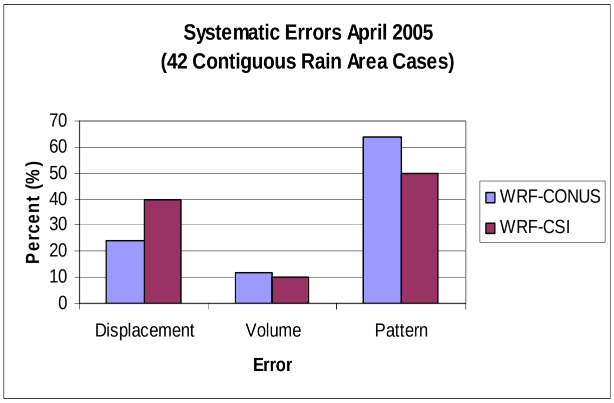

Figure 3. Systematic error contribution of 42 Contiguous Rain Areas for WRF-CONUS and WRF-CSI.

forecasts. However, it appears that the WRF-CONUS does hold a slight statistical advantage in each of the aforementioned variables. Precipitation verification shows that while both models exhibit high rates of detection, their forecast behavior is quite different. Whereas the WRF-CONUS forecasts larger, or more synoptic scale, precipitation entities more accurately, the WRF-CSI demonstrates skill with smaller CRAs. This detection rate for the WRF-CSI may prove to be beneficial during the summer months for sea breeze convection. However, more testing and verification is certainly needed, namely for warm season precipitation, before any conclusions can be made pertaining to any added benefits of an extended domain.

V. References

Bogenschutz, P. A., Ruscher, P., and P. Welsh, 2005: Skill of the new Weather Research and Forecast model on warm season precipitation in the southeast United States. *Mon. Wea. Rev.* (submitted).

Bogenschutz, P., P. Ruscher, P. Welsh, J. Mahoney, J.A. McGinley, M. Kay, B. Shaw., J. Smart, J. Savadel, and J. McQueen, 2004: Summer season verification of the first NWS operational WRF model forecasts from the NOAA Coastal Storms Initiative project in northeast Florida. *20th Conf. On Wea. Anal. and Forecasting/16th Con. On NWP,* Seattle, WA. Amer. Meteor. Soc. CD-ROM, J12.1.

Case, Jonathan L., Manobianco, John, Dianic, Allan V., Wheeler, Mark M., Harms, Dewey E., Parks, Carlton R., 2002. Verification of high-resolution RAMS forecasts over east-central Florida during the 1999 and 2000 summer months. *Wea. and Forecasting*, **17,** 1133–-1151.

Chuang, H., G. DiMego, M. Baldwin, and WRF DTC team, 2004. The NCEP WRF post-processing software. *The Joint WRF/MM5 Users Workshop*, Boulder, CO.

Ebert, E.E. and J.L. McBride, 2000. Verification of precipitation in weather systems: determination of systematic errors. *J. Hydrol.*, **239**, 179-202.

Janjic, Z. I., 2003. A nonhydrostatic model based on a new approach. *Meteorol. Atmos. Phys*. **82**, 271-–285.

Nance, L., L. Bernardet, H. Chuang, G. DiMego, M. Demirtas, R. Gall, S. Koch, Y. Lin, A. Loughe, J. Mahoney and M. Pyle, 2005. The WRF Developmental Testbed Center: A status report. The Joint WRF/MM5 Users Workshop, Boulder, CO.

Shaw, B., Welsh P.T.,A. Wildman, J. Smart, P. Ruscher, J. Savadel, J. McGinley, M. Kay, J. Mahoney, J. McQueen, 2004. Applying the Weather Research and Forecasting (WRF) model to National Weather Service Forecast Office operations. *Preprints 20th Conf. On Wea. And Forecasting/16th Conf. on NWP,* Seattle, WA, Amer. Meteor. Soc. *CD-ROM, 1.2.*